Bažant, Z.P., Kim, J.-J., and Li, Y.-N. (1995). "Part-through bending cracks in sea ice plates: Mathematical modeling." in *AMD-Vol. 207, Ice Mechanics* (ASME Summer Meeting, Los Angeles, CA, June 1995), ed. by J.P. Dempsey and Y. Rajapakse, 97-105.

AMD-Vol. 207

ICE MECHANICS
– 1995 –

Presented at

THE 1995 JOINT ASME APPLIED MECHANICS AND MATERIALS SUMMER MEETING
LOS ANGELES, CALIFORNIA
JUNE 28–30, 1995

Sponsored by

THE APPLIED MECHANICS DIVISION, ASME

Edited by

J. P. DEMPSEY
CLARKSON UNIVERSITY

Y. D. S. RAJAPAKSE
OFFICE OF NAVAL RESEARCH

THE AMERICAN SOCIETY OF MECHANICAL ENGINEERS
345 East 47th Street ■ United Engineering Center ■ New York, N.Y. 10017

AMD-Vol. 207, Ice Mechanics
ASME 1995

PART-THROUGH BENDING CRACKS IN SEA ICE PLATES: MATHEMATICAL MODELING

Zdeněk P. Bažant, J.J.H. Kim and Yuan N. Li
Department of Civil Engineering
Northwestern University
Evanston, Illinois

ABSTRACT

The paper presents a new mathematical model for propagation of part-through bending cracks in floating sea ice plate, which is a problem of considerable practical importance, for example, the load carrying capacity or penetration through the ice plate. After reviewing the previous work on propagation of through-cracks due to transverse loads, the three-dimensional problem of part-through cracks is simplified as two-dimensional using the well known approximation by line springs. These nonlinear springs describe the relation of rotation and additional in-plane expansion due to part-through crack to the bending moment and normal force transmitted through the crack. The problem of several radial cracks emanating from a small loaded area is analyzed. The bending and in-plane elastic responses of the floating plate are described by compliance functions. It is shown that the rotations across the crack cause the compression resultant in the plates and the neutral axis of the stress to shift above the mid-thickness of plates. This represents a dome effect which carries a significant part of the load. The profile of the crack depth propagating upward and the shape of the dome are calculated. A study of the failure loads and the size effect is left for a subsequent paper.

INTRODUCTION

Sea ice plates under vertical loading from above or from below often fail by propagation of radial cracks from the loaded area (Fig. 1). The maximum or failure load is reached when circumferential cracks start to form from the radial cracks. This type of failure is important for many commercial as well as defense applications, such as a submarine sail penetrating through the ice or an airplane landing on the ice. Due to these practical needs, this problem has been studied extensively for a long time. However, due to the relatively recent initiation of fracture mechanics of ice, the problem has been solved using a strength criterion or plastic limit analysis. Obviously, since ice is a quasibrittle material, the plastic limit analysis is unrealistic and more importantly, it does not capture the size effect on the nominal strength.

In early studies of the penetration problem, the load capacity of a floating ice plate was determined by the tensile strength criterion (e.g. Bernstein, 1929). Nevel (1958) analyzed the strength of the ice plate assuming that the number of radial bending cracks is very large and that the ice plate is thus split into wedges of very small angle, which can be treated as beams of variable cross section. An excellent review of the early studies of the load capacity of the floating ice plate was given by Kerr (1975).

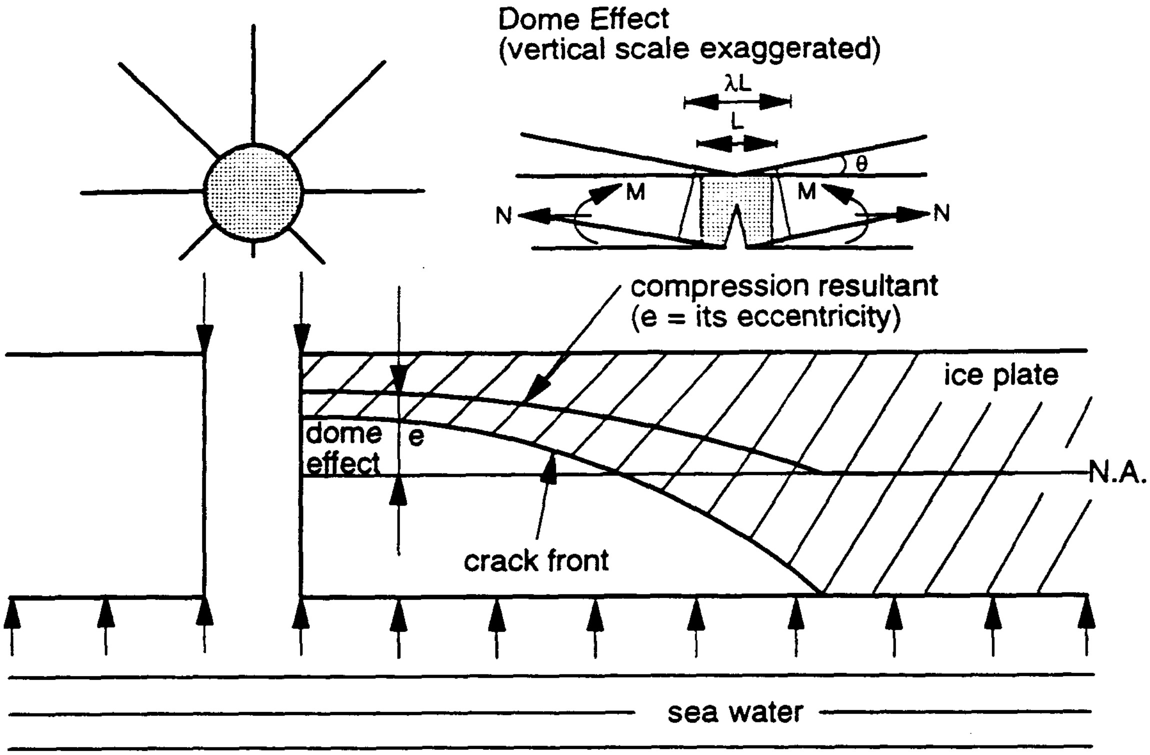

Figure 1. Sea ice plate model.

Recently, fracture mechanics has been applied to solve the penetration problem. There are two reasons for introducing fracture mechanics. One reason is that the ice plate dose not fail until extensive radial cracks develop. The other reason is that there is size effect on the penetration load. Without fracture mechanics, our knowledge of size effect would be inadequate.

To accurately account for the effect of the radial bending cracks, linear elastic fracture mechanics (LEFM) was introduced by Bažant and Li (1994) to study the relation between the applied load and the length of radial cracks. Later, Li and Bažant (1994) studied the problem of how to determine the number of radial cracks. In these studies, which are reviewed in the first part of this paper, the radial cracks were assumed to be fully opened through-cracks. Interaction between the neighboring wedges across part-through cracks was neglected. Horizontal expansion which is associated with bending cracks causes the cracks to open only through part of the thickness of the plate, which was observed by Frankenstein (1963). This expansion induces compressive forces in the plate and thus engenders a dome effect, which plays an important role in helping to carry the vertical load.

A plate with part-through cracks is actually a three-dimensional problem. However, based on the simplifying idea of an embedded line spring, proposed by Rice and Levy (1972) in a study of fracture of metal plates, the problem can reduced to a two-dimensional one. Since the depth of radial bending crack opening is unknown in advance, the compliances of the line springs are unknown functions and have to be solve together with the plate problem. The set of integral equations based on the compliance influence functions has been proposed be Bažant and Li (1995) to determine the stress distribution along the partially cracked surfaces if the crack front profile is known. The criterion proposed by Bažant and Li (1995) for crack depth determination, however, needs to be modified to circumvent the difficulties associated with the crack initiation. A numerical solution of the problem will be described to reveal the main features of crack growth as well as stress distribution. The dome effect of the plate under vertical loading will be demonstrated.

LINEAR FRACTURE MECHANICS OF SEA ICE PLATE WITH THROUGH-CRACKS

In this section, the linear elastic fracture mechanics analysis of sea ice plate will be briefly reviewed for the purpose of comparison with the subsequent modeling effort. The basic assumptions as well as some new terminologies are introduced and defined throughout the presentation.

Consider an infinitely extending elastic plate of thickness h floating on water of specific weight ρ. The water acts exactly as an elastic foundation of Winkler type. The differential equation of equilibrium of the plate in terms of the vertical downward deflection in rectangular coordinates x, y may be written as

$$D\left(\frac{\partial^2}{\partial x^2}+\frac{\partial^2}{\partial y^2}\right)\left(\frac{\partial^2 w}{\partial x^2}+\frac{\partial^2 w}{\partial y^2}\right)+\rho w=0 \tag{1}$$

when $D = Eh^3/12(1-\nu^2)$ = cylindrical stiffness of the elastic plate of thickness h, ν= Poisson's ratio, E = Young's modulus, and h = plate thickness. We have assumed implicitly that the load is applied only on the boundary of the plate.

It is convenient to introduce a length constant for the plate as $L=(D/\rho)^{1/4}$;L may be called the flexural wavelength and it also represents the length over which an end disturbance in a semi-infinite plate decays to e^{-L} of the end value. Using the non-dimensional coordinates $X = x/L$ and $Y = y/L$, we can write the governing differential equation of a plate resting on elastic foundation as:

$$\left(\frac{\partial^2}{\partial X^2}+\frac{\partial^2}{\partial Y^2}\right)\left(\frac{\partial^2 w}{\partial X^2}+\frac{\partial^2 w}{\partial Y^2}\right)+w=0 \tag{2}$$

The conjugate displacement of the applied load can be written as $w = PL^2F(\alpha,n)/D$, if P is the only external force that is applied to the plate; $\alpha = a/L$ is the non-dimensional radial crack length and n is the total number of radial cracks which are assumed to distribute uniformly around the loading circle. Such an assumption is implicitly assumed in the previous analyses (Bažant and Li, 1994; Li and Bažant, 1994). The load level is determined by the condition that the rate of external work done by the applied load be completely converted into the surface energy of the ice plate, or expressed as

$$\frac{P}{2L}\frac{\partial w}{\partial \alpha}=\frac{P^2L}{2D}\frac{\partial F(\alpha,n)}{\partial \alpha}=nhG_f \tag{3}$$

In other words, once we know the function $F(\alpha,n)$, the applied load P is readily solved for any given radial length.

Eq. 3 constitutes the foundation of our previous fracture mechanics analysis of the ice plate. If the radial crack does not cut fully through the thickness, then Eq. 3 is no longer valid for two reasons: First, the surface energy required to extend the radial cracks by a unit length cannot be simply written as nhG_f. Second, the work done by the external load can no longer be expressed as $(P/2L)(\partial w/\partial\alpha)$. Most importantly, the shape of the radial crack frontal profile must be determined by some additional condition. Therefore, fracture mechanics analysis of a plate with part-through cracks must be quite different from the simple approach reviewed in this section.

STRESS ANALYSIS OF ICE PLATE WITH PART-THROUGH RADIAL CRACKS

The assumption that the surfaces of radial cracks are free from stress is, indeed, a very crude approximation. If the load is applied on the top of the ice plate, the top portion of the plate is under horizontal compression. In the field, radial cracks manifest themselves as a whitening on the top surface of the ice (Frankenstein, 1963), and they usually become apparent only after the load is removed. In other words, the radial cracks are opened only in the lower part of the plate while the upper surfaces remain closed due to the compression generated by the applied load. This tends to produce in-plane compression forces in the plate, whose resultant is shifted above the mid-thickness. Thus a dome effect develops and helps to carry the load. The previous analyses ignored the dome effect.

The partial opening of the radial cracks is a three-dimensional phenomenon. A detailed three-dimensional fracture mechanics analysis is computationally expensive, if not intractable. In the present analysis, it is proposed to model the partial crack as a line spring in the crack line. Within this framework, the plate with

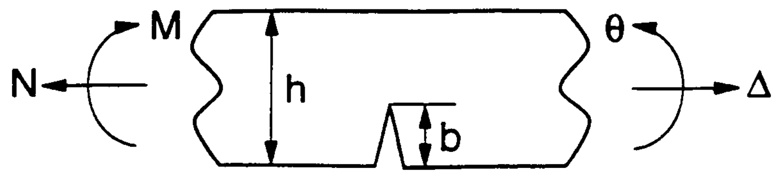

Figure 2. Resultant forces and displacements.

radial cracks, floating on water, can still be analyzed as a two dimensional problem. The effect of partial cracking in the plate is reflected by its increased compliance, which is represented by line springs.

The idea of incorporating the compliance increase of plates due to the presence of part- through cracks was proposed by Okamura et al. (1972). Rice and Levy (1972) used the same idea to solve the stress intensity factors of a partially cracked plate subjected to in-plane and out-of-plane loads. In their paper, they stated various assumptions involved in such an approach to solve part-through surface cracks of given crack depth profile. Our problem, however, is quite different. The crack depth, or the crack frontal profile of the radial cracks, is not known in advance. Determination of the radial crack profile is part of the problem.

Denote by Δ the additional crack expansion (in circumferential direction) and θ the additional crack surface rotation (about the radial ray) due the presence of the crack; Δ and θ vary with radial distance r and the variation is unknown in advance. Denote by N and M the normal force (force per unit length) and bending moment (moment per unit length) associated with Δ and θ (Fig. 2). A positive moment causes tension in the bottom surface of the plate, and a tensile normal force is taken as positive. Furthermore, denote by $b(r)$ the depth of the radial cracks at position r. Since we have replaced the partially cracked surfaces with line springs, the surface forces and the surface displacements can be written as

$$\Delta = \lambda_{11} N + \lambda_{12} M \qquad \theta = \lambda_{21} N + \lambda_{22} M \tag{4}$$

The compliances λ_{ij} (i, j=1,2) of the line springs can be expressed in terms of the stress intensity factors (SIF) as

$$\lambda_{ij} = 2\frac{1-\nu^2}{E}\int_0^b k_i(t)k_j(t)dt \tag{5}$$

k_i (i=1,2), where k_1 = SIF in an infinite strip of height h with a single-sided notch of depth b, loaded remotely by a unit N, and k_2 = SIF of the same strip loaded by a unit M. Approximate expressions for λ_{11} and λ_{22} are given by Tada et al. (1985), and so only an empirical formula for λ_{12} needs to be calibrated through Eq. 5.

The rotation and expansion are related to the elastic solution of the ice plate (which has n radial cracks of length a) as follows

$$\theta(r) = C_{MP}(r)\frac{P}{n} - \int_0^a C_{MM}(r,r')M(r')dr' \tag{6}$$

$$\Delta(r) = -\int_0^a C_{NN}(r,r')N(r')dr' \tag{7}$$

where $C_{MP}(r)$ is the rotation of the plate at r due to a unit P, $C_{MM}(r,r')$ is the rotation of the plate at r due to a unit moment acting on the crack surfaces at r', and $C_{NN}(r,r')$ is the crack expansion at r due to a unit normal force N at r'. The compliance functions are calculated for a wedge plate (Fig. 3) with $b(r) = 1$ for $a_0 \le r \le a$, and $b(r) = 0$ for $r > a$. The interaction in the radial cracks is ignored. The negative sign in front of the integrals is due to the fact that positive forces on the crack surfaces cause the crack to close. All these compliance influence functions can be solved by numerically, e.g., by the finite element method or finite difference method.

Substituting Δ and θ from Eq. 4 into Eqs. 6 and 7, one obtains the following integral equations:

$$\lambda_{21}(r)N(r) + \lambda_{22}(r)M(r) = C_{MP}(r)\frac{P}{n} - \int_0^a C_{MM}(r,r')M(r')dr' \tag{8}$$

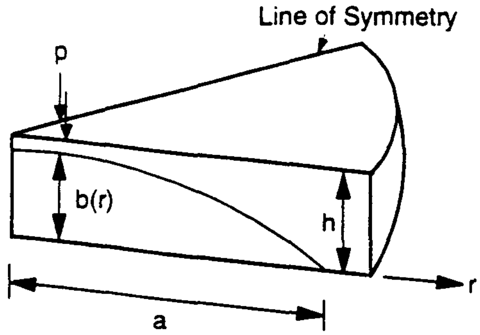

Figure 3. Radial crack depth profile.

$$\lambda_{11}(r)N(r) + \lambda_{12}(r)M(r) = -\int_0^a C_{NN}(r, r')N(r')dr' \tag{9}$$

These equations can be used to solve for the unknown functions N and M along the radial crack surfaces if the radial crack depth as well as the applied load P are known, although the radial crack profile as well as the applied load are yet to be determined at this stage. In particularly, these two equations can also be used to determine M and N where the crack depth is zero.

GENERALIZED STRENGTH CRITERION

It can be seen that the internal forces M and N can be determined if the crack frontal profile and the applied load P are known. To close the formulation, one may postulate, as was done by Bažant and Li (1995), that at any point along the radial cracks the total stress intensity factor at the crack tip be equal to K_f, the fracture toughness of the ice. That is:

$$k_1[b(r)]N(r) + k_2[b(r)]M(r) = K_f \qquad a_0 \le r \le a \tag{10}$$

The fracture energy G_f and the fracture toughness K_f are related by the equation $G_f = K_f^2(1-\nu^2)/E$. However, this equation cannot be applied if $b = 0$, because the stress intensity factors k_1 and k_2 are zero. When k_1 and k_2 are zero, Eq. 10 cannot be satisfied, no matter how large the internal forces M and N become. In other words, the crack cannot get started if there is no initial notch. Obviously, this limitation is inherited from linear elastic fracture mechanics, which can only be applied to a structure in which there is already a crack.

To establish the crack initiation load, a conventional strength criterion could have been employed. Such a criterion, however, would become invalidated once there is a crack in the structure, because the stress at the crack tip becomes infinite and the conventional strength criterion would predict crack growth for infinitesimal load level, which is also unacceptable.

The true behavior of ice without an initial crack in a tensile stress zone is quite complicated. When the stress level is raised to certain value, initially there would be diffusive cracks of sizes comparable to the microscopic features such as the grains of the ice. These microscopic cracks interact with each other and compete for energy to grow. Only those located in a good position and oriented in a favorable direction can grow faster than the other cracks. As a result, only few cracks will eventually grow to macroscopic sizes and become dominant. One can easily see that the appearance of a macroscopic crack from a smooth surface is a highly nonlinear process. Although some simple relations that govern the emergence of cracks from smooth surfaces have been discussed by Li and Bažant (1994,1995), much remains to be learned. In addition, those studies have focused on the pattern of the radial cracks emanating from a smooth hole, rather than on individual cracks.

What we need in this analysis is a strength criterion that can be used with or without a crack. .The generalized strength criterion to be discussed in this paper is inspired by Bažant's size effect formula, which has a general form as

$$\sigma_M = \frac{Bf_t'}{\sqrt{1 + \frac{h}{D_0}}} \tag{11}$$

where σ_M is the nominal stress of the load, f_t' is the tensile strength of the material under direct tension, and D_0 is a measure of material brittleness which, although size-independent, depends on the geometry (such as crack depth) of the structure under consideration. B is a constant that is related to the way the nominal stress is defined. This equation states that when the structure is very large (i.e., the structure size h is much larger than D_0), then the nominal strength of the material is determined by linear elastic fracture mechanics. This means that the nominal strength scales with the inverse square root of h. On the other hand, if h is much smaller than D_0 then the conventional strength criterion, which is size independent, becomes dominant. Such a transitional behavior is typical of quasibrittle materials, and Eq. 11 has been proved to reproduce many experimental results with very reasonable accuracy.

If we write a general stress intensity factor as $K = \sigma\sqrt{b}f(b/h)$ (where the function f is non-dimensional), then the corresponding energy release rate can be written as $G = (1-\nu^2)\sigma^2 hg(b/h)/E$, with the non-dimensional function $g(b/h) = (b/h)f^2(b/h)$. It can be easily shown that $D_0 = l_0/[B^2g(b/h)]$ ($l_0 = EG_f/f_t'^2(1-\nu^2)$ which is the material length of the ice), and Eq. 11 is the same as the strength criterion dictated by linear elastic fracture mechanics if the structure size (measured by the thickness h herein) is sufficiently large when compared with D_0. It is important to realize that the largeness or smallness of structure size is based on the ratio of h and D_0. When parameter D_0 changes, the relative largeness or smallness of h also changes even though h itself does not change. More specifically, when crack depth ratio b/h is small, D_0 is large, thus causing the conventional strength criterion to be dominant. On the other hand, if b/h is close to 1, then D_0 becomes very small, thus linear elastic fracture mechanics governs the behavior. In other words, Eq. 11 contains, naturally, the smooth transition from the conventional strength criterion to the linear fracture mechanics strength criterion, when h is constant while the relative crack depth b/h increases from 0 to 1.

The actual strength criterion adopted in this analysis is a slightly modified equation. Modification is necessary because there are more than one force acting on the plate. Denote $\sigma_M = 6M/h^2$ and $\sigma_N = N/h$ the nominal stresses corresponding to M and N. Then the generalized strength criterion can be expressed as

$$\sigma_M = Bf_t'\left[1 + (B^{2r} - 1)\frac{h^*}{1+h^*} + (B^2 g(\frac{b}{h}, \frac{\sigma_N}{\sigma_M})h^*)^r\right]^{-\frac{1}{2r}} \tag{12}$$

where $B = 3(1 - \sigma_N/f_t')$ is the plastic limit (assuming the compressive strength of the ice is large enough compared to its uniaxial direct tensile strength f_t' so that we can assume it to be infinite). The nondimensional structure size $h^* = h/l_0$.

The second term in the denominator is introduced to take into account the rupture modulus of the plate under bending. It is known that the rupture modulus is size dependent. For very small size h^* the rupture modulus is close to its plastic limit value introduced by the non-dimensional number B. On the other hand, for very large h^*, the rupture modulus of bending becomes the same as the direct uniaxial tensile strength f_t' of the material. Obviously, Eq. 12 satisfies these requirements. So it will replace Eq. 10 as the strength criterion to determine the crack depth profile.

The parameter r is introduced to adjust the shape of the generalized strength criterion such that a better correlation with experimental data, if available, could be achieved. In this analysis we use the value $r = 0.7$. The function g is defined as

$$g\left(\frac{b}{h}, \frac{\sigma_N}{\sigma_M}\right) = \frac{b}{h}f^2\left(\frac{b}{h}\right) = \frac{b}{h}\left[f_2\left(\frac{b}{h}\right) + \frac{\sigma_N}{\sigma_M}f_1\left(\frac{b}{h}\right)\right]^2 \tag{13}$$

where the nondimensional function $f = f_1 + f_2$ is defined by the following relations:

$$k_1\left(\frac{b}{h}\right) = \frac{1}{h^2}\sqrt{b}f_1\left(\frac{b}{h}\right) \qquad k_2\left(\frac{b}{h}\right) = \frac{6}{h^3}\sqrt{b}f_2\left(\frac{b}{h}\right) \tag{14}$$

SOLUTION OF ICE PLATE WITH PART-THROUGH RADIAL CRACKS

The basic unknown quantities in the problem of ice plate with part-through radial cracks are the applied load P, the internal forces $M(r)$ and $N(r)$ that act across the radial crack surfaces, and the crack depth profile $b(r)$. The three unknown functions can be determined by Eqs. 8-9 and 12. The load level P is also determined by Eq. 12. This is because, for a radial crack with its total length denoted by a (or in its non-dimensional form $\alpha = a/L$), the stress level at the bottom surface along the radial line, where $r = a$, must be less than the tensile strength of the ice, which is given by the Eq. 12 with $b = 0$. If the stress is greater that the strength, than the radial crack will extend under that load level.

One must inevitably resort to numerical means to solve these nonlinear equations. In the numerical example to be described later, the plate is described by a mesh that consists only of radial rays and circumferential arcs. Using the finite difference method or the finite element method, we can calculate the compliance functions $C_{MP}(r)$, $C_{MM}(r, r')$, and $C_{NN}(r, r')$ as matrices. Since the radial crack length can only assume values compatible with the selected mesh, it is found to be more convenient to use a as a basic parameter in the calculation. The load P is solved as an unknown.

However, when the length of radial crack is sufficiently long, the the compressive stress σ_N becomes enormous due to the dome effect. In other words, the ratio σ_N/σ_M will become a substantially negative number. When this happens, function f, which is proportional to the total stress intensity factor K, will become negative. When K is negative, the crack will not grow no matter how large σ_N and σ_M is (as long as they keep the same ratio), and the generalized strength criterion becomes invalidated, although it remains defined mathematically. Whenever K is negative, Eq. 12 shall be replaced by the equation

$$f\left(\frac{b}{h}\right) = f_2\left(\frac{b}{h}\right) + \frac{\sigma_N}{\sigma_M} f_1\left(\frac{b}{h}\right) = 0 \qquad (15)$$

With this stipulation, we have completed the mechanical formulation of ice plate with part-through radial cracks.

NUMERICAL EXAMPLE

To illustrate the main features of the model proposed in this research, a numerical analysis was done on an ice plate with six 60° angular wedges. This means that the six total part-through radial cracks will form around the small circular area of loading. Due to the symmetry of the structure along the center line of a single wedge, the analysis only dealt with a half wedge with 30° central angle. The parameters used in the analysis were $f_t' = 0.2$ MPa, $\rho = 9810$ N/m^3, $\nu = 0.29$, $E = 1.0$ GPa, $K_c = 0.1$MN m$^{-3/2}$, $G_f = 10$ N/m, the nondimensional maximum radial crack length = $3.0L$, the nondimensional radius of the circular loaded area = $0.1L$, and the nondimensional thickness of the ice plate = $0.1L$. L is the flexural wavelength of ice. The mesh size used in the analysis was 20 uniform angular nodes and 30 non-uniform radial nodes. The radial nodes were positioned so that the mesh was fine near the loaded area and gradually getting coarser away from it.

The solution is summarized in Fig. 4. Each line in these plots represents the distribution of the unknown quantity for a given radial crack length a. There are three different phases in the analysis. Initially, as the radial crack lengthens, the maximum nondimensional resultant moments and normal forces gradually increase from the first node to the node at which the radial crack length has been reached. Also note that the maximum moment at the tip of the radial crack is about $1.8L$ and the values of the normal forces are negligible. The crack depth gradually increases as the crack length increases and the crack edge has a descending slope. The initial results are similar to what would have been expected before the analysis. However, as the radial crack length increases to a sufficient length, a moderate change occurs in the profile of the resultant moment. The moment profile changes its shape from a gradually ascending profile to a valley-shaped profile. Unlike the deviation in the profile of the resultant moment, the profile of the normal forces and the crack depth continue as before. This variation is caused by the continuous increase of the normal forces in the nodes behind the crack front. In order to neutralize the increasing normal forces, the moments increase such that the node at which the maximum moment resides is not the node with a largest crack depth.

A more dramatic change occurs when the nondimensional radial crack length equals approximately $0.9L$. At this point of the analysis, the nondimensional moment at the first node was about $2.3L$ and the

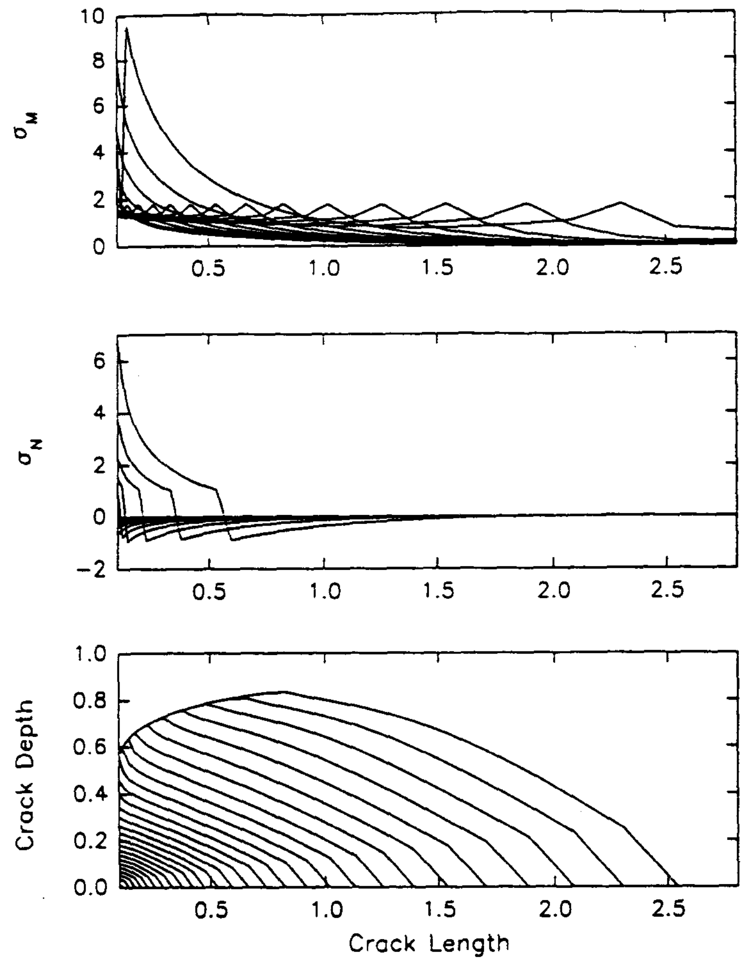

Figure 4. Numerical results.

convergence of the equations becomes very difficult. Mathematically, this is equivalent to getting a negative value for the term $f_2 + (\sigma_M/\sigma_N) f_1$. The phenomenon of getting a negative stress intensity factor in front of the crack tip is physically inadmissible and therefore Eq. 12, which is a crack growth condition, is replaced with Eq. 15. With this replacement, the analysis is able to continue until the radial crack length reaches the preset maximum length.

As soon as Eq. 15 is implemented at the affected nodal points, the results change dramatically. The crack depth profile changes from a shape with a gradually descending slope to a crest shape. Note that Eq. 15 requires only the total stress intensity factor to be zero if no positive value is possible. This condition can be achieved by changing the stress ratio or shortening the crack depth. However, our calculation indicates that the shortening of the crack depth did not actually happen. Once the depth reaches its maximum value, it stays at the same value. In other word, the shape of the maximum crack depth is preserved and would not change by a further lengthening of the total radial crack length.

Since the portion of radial crack where the crack depth is maximized is associated with large compressive stress, the neutral axis is significantly shifted upward, as is shown schematically in Fig. 1. This upward shift of the neutral axis (or neutral surface) is a manifestation of the dome effect, which has been ignored in previous analysis. The inclusion of the dome effect in the analysis will certainly change the relation between the load level P and the total radial crack length a. The calculation of the failure load by the formation of a circumferential crack is still in progress at this moment and therefore is not included in the example. Since the relation between P and a is significantly changed, we expect the final failure load will also be changed. The result, however, will be published elsewhere.

ACKNOWLEDGEMENT

Financial support under grant N00014-91-J-1109 (monitored by Dr. Y. Rajapakse) from the Office of Naval Research to Northwestern University is gratefully acknowledged.

REFERENCES

Bažant, Z.P., and Cedolin, L., 1991, *Stability of structures: Elastic, Inelastic, Fracture and Damage Theories*, Oxford University Press, New York.

Bažant, Z.P., 1992, "Large scale thermal bending fracture of see ice plate," *J. Geophysical Research Oceans*, Vol. 97 (C11), pp. 17739–17751

Bažant, Z.P. and Li, Y.N., 1994, "Penetration Through Floating Sea Ice Plate and Size Effect: Simplified Fracture Analysis," in press, *J. Engng. Mech. ASCE*, No. 7, pp. 1304–1321

Bernstein, S., 1929, "The railway ice crossing" (text in Russian), *Trudy Nauchno-Technicheskogo Komiteta Narodnogo Komissariata Putei*, Soobshchenniia, Vol. 84 (in Russia).

Frankenstein, E.G., 1963, "Load test data for lake ice sheet," *Technical Report 89*, U.S. Army Cold Regions Research and Engineering Laboratory, Hanover, New Hampshire.

Kerr, A.D., 1975, "The bearing capacity of floating ice plates subjected to static or quasi-static loads – A critical survey," *Research Report 333*, U.S. Army Cold Regions Research and Engineering Laboratory, Hanover, New Hampshire.

Li, Y. N. and Bažant, Z.P., 1994, "Penetration fracture of floating ice-plate: 2D analysis and size effect," *J. Engng. Mech. ASCE* 120, No. 7, pp. 1481–1498

Nevel, D.E., 1958, "The theory of narrow infinite wedge on an elastic foundation," *Transactions, Engineering Institute of Canada*, Vol. 2, No. 3.

Okamura, H., Watanabe, K., and Takano, T., 1972, "Applications of the compliance concept in fracture mechanics," in 6th National Symposium on Fracture Mechanics, Progress in Flaw Growth and Fracture Toughness Testing, *ASME Special Technical Publication No. 536*, pp. 423–439.

Rice, J.R. and Levy, N., 1972, "The part-through surface crack in an elastic plate," *J. Appl. Mech. ASME*, Vol. 39, pp. 185–194.

Tada, H., Paris, P.C., and Irwin, G.R., 1985, *Stress analysis of cracks handbook*, Del Research Corp., Hellertown, PA.